

SYNCHRONIZED STEP MULTILEVEL MARKOV CHAIN MONTE CARLO*

SANJAN MUCHANDIMATH[†] AND ALEX GORODETSKY[†]

Abstract. In this work, we propose a new algorithm for coupling Markov chains in a Markovian multilevel Monte Carlo estimator. We apply this approach for solving Bayesian inverse problems that consist of multiple model fidelities. The coupling methodology, termed as synchronized step correlation enhancement (SYNCE), is inspired by the concept of using common random numbers in Markov chain Monte Carlo sampling. This methodology is shown to be more efficient and cost-effective than existing couplings in the literature. This improvement is achieved because SYNCE leads to higher correlation of samples obtained from level dependent posteriors than previous works. SYNCE is especially effective at coarse levels of the hierarchy where posteriors differ significantly from each other, resulting in orders of magnitude improvement in variance reduction. We first demonstrate the effectiveness of our proposed methodology by comparing it with existing algorithms on two simple examples taken from the literature. We then apply our methodology to a more complex example in the context of uncertainty quantification in subsurface flow simulations.

Key words. Markov chain Monte Carlo, Bayesian inverse problems, multilevel Monte Carlo, multi-fidelity, coupling

MSC codes. 62F15, 62M05, 65C05, 65C40

1. Introduction. Bayesian inference is a well established technique for estimating parameters of complex mathematical models. In this stochastic framework, the parameters θ of a model \mathcal{F} are modeled as random variables. A prior $\pi^0(\theta)$ is assigned and the posterior $\pi(\theta | y_{\mathcal{D}})$ is obtained using Bayes rule given observed data $y_{\mathcal{D}}$. Given a distribution over the parameters, application goals typically seek to estimate statistics of some output functional Q ; for example, to compute the expectation $\mathbb{E}_{\theta \sim \pi(\theta | y_{\mathcal{D}})}[Q(\theta)]$. Moreover, for non-linear and non-Gaussian settings, such estimation is typically done via a Monte Carlo estimator with N samples.

Markov chain Monte Carlo (MCMC) methods are typically used to generate the samples [32, 15]. These approaches are able to solve highly complex problems, but their computational cost is often prohibitive because the $1/N$ reduction rate in error necessitates a large number of samples from the posterior and forward evaluations of Q . More specifically, the computational tractability of obtaining a good estimate depends on two factors: the cost of evaluating the functional quantity Q for a given sample and the cost of sampling from the posterior distribution $\pi(\theta | y_{\mathcal{D}})$. When the prediction model is time-consuming, evaluating Q many times is expensive. Furthermore, when the likelihood model \mathcal{F} is computationally intensive, then generating samples of $\pi(\theta | y_{\mathcal{D}})$ is also time-consuming.

Multi-fidelity strategies have been developed to alleviate these computational costs [29], and this paper seeks to improve these strategies for inverse problems. Multi-fidelity strategies combine outputs from models of varying complexity to achieve computational speedups while preserving accuracy. Two key requirements for these methods are: (1) the availability of both low-fidelity (less accurate but computationally cheap) and high-fidelity (more accurate but computationally expensive) models,

*Submitted to the editors on January 27th, 2025.

Funding: This work was funded by the Aeronautics Research Mission Directorate at NASA through the Transformative Aeronautical Concepts Program (TACP) and the D.2 Transformational Tools and Technologies Project (TTT) under contract no. 80NSSC23M0215.

[†]Department of Aerospace Engineering, University of Michigan, Ann Arbor, MI 48105, USA (sanjanm@umich.edu, goroda@umich.edu)

and (2) a model management strategy that distributes work/samples among these available models. Low-fidelity models can arise from either approximations to the same underlying physical model or by employing coarse grid approximations. For example, physical processes (for example fluid flow) are modeled as partial differential equations (PDE's) with spatial and/or temporal derivative terms. Numerical methods are employed to discretize the PDE's with a certain resolution (for example the mesh size). Increasing the resolution will lead to a more accurate output but at the expense of a higher cost compared to an evaluation with a lower resolution.

Multi-fidelity sampling techniques have been extensively explored over a long history as part of model management strategies through the lense of control variate (CV) [24, 15, 8, 10] techniques. When modified to the sampling context, approximate control variate (ACV) [13, 30] techniques use the low fidelity models as control variates to reduce the variance of the estimator. Multilevel Monte Carlo (MLMC) [17, 12, 6, 25] is a commonly used special case of the approximate control variate framework obtained by enforcing a telescoping sum and setting the control variate weights to -1. The magnitude of variance reduction in these frameworks depends on the *correlation* between the functional quantities of the low and high-fidelity models, with higher correlations leading to higher variance reduction.

The inverse problem we consider here has an additional degree of freedom compared to the standard way multi-fidelity sampling approaches are used for forward problems. Namely, the *generation* of the input samples themselves is expensive. For example, in classical MLMC, all the models are assumed to share a common set of uncertain variables. However, in the inverse context, we have an additional opportunity to reduce the computational cost of generating samples by appealing to *low-fidelity posteriors*. Instead of performing standard multi-fidelity forward UQ with samples from the high-fidelity posterior, there is an opportunity to mix and match posteriors of various model fidelities. However, this opportunity comes with some additional challenges. If the input distributions to each model fidelity can potentially be different, how do we ensure that high correlations are maintained?

Solutions to this problem can be addressed within the framework of *coupled Markov chains*. Coupling in this context refers to the idea of creating a joint Markov kernel that induces a Markov chain on the product space of the individual chains such that the marginals of the joint chain are the target distributions of the individual chains. Couplings can be used to correlate the samples obtained from the different levels of a model hierarchy to improve the convergence of the combined algorithm.

Several existing works have proposed different coupling methods. The authors in [7] use the idea of proposing a point from the coarse chain as a candidate for the fine chain. This idea was previously explored in detail by the authors in [5], where they provided some bounds on the closeness of the posteriors for their framework to be effective. Note that samples are proposed from an approximation to the true coarse posterior leading to bias in the estimator [7, 23]. The authors in [21] expand on the coarse proposal idea to create ergodic chains by using recursivity and an adaptive delayed acceptance framework. Independent proposals are explored in [23] where chains are coerced to accept the same proposed point from the sampler. The authors also provide restrictive conditions on the proposal for the chains to be ergodic. To leverage state dependent proposals, the same authors in [22] introduce the maximal coupling method in the MLMC framework. Recently, other interesting applications of coupling have been applied to create unbiased estimators [19, 18]. Existing methodologies improve correlation of the output functionals by forcing the coarse and fine chains to accept the same proposed point. However, these methods are not always

effective, especially when the posteriors at different levels are significantly different, necessitating the need for a more robust coupling methodology.

Couplings have been explored in the context of uncertainty quantification (UQ) for forward problems as well. The authors in [11] leveraged multi-fidelity techniques to define a shared space among all models using active subspaces. The authors in [20] employ multi-fidelity techniques to reduce the computational cost of performing dimension reduction through the gradient-based active subspace method. In [4], the authors proposed a multi-fidelity coupled uncertainty propagation method using adaptive sampling strategies. These works show how the efficiency of even forward UQ methods can be tuned to increase the correlation between the different fidelities — that good approaches to coupling can be used to improve correlation.

The key contributions of this paper are:

1. We review existing methodologies for integrating MCMC with the MLMC estimator and provide insights into how these methods come under the framework of Markov chain coupling.
2. We introduce a novel method called SYNCE coupling, inspired by [31]. Additionally, we propose an adaptive version, SYNCE-AR that works by adapting and resynchronizing the coupled kernel.
3. We demonstrate that our proposed methodology is more efficient than existing couplings in the literature, achieving an order or two gain in variance reduction. This is possible because of higher sample correlation across level-dependent posteriors, particularly at coarse hierarchical levels where posteriors significantly differ.

The rest of the paper is structured as follows: In subsection 2.1, we will discuss the Bayesian inverse problem in hand and review standard MCMC methods used to solve these problems. We will then introduce the control variate and approximate control variate frameworks in subsection 2.2. Couplings and their extensions to Markov chains are explored in subsection 3.1. Existing couplings for the multilevel Markov chain Monte Carlo estimators are discussed in subsection 3.3 and our proposed methodology is explained in detail in section 4. We will then present numerical results in section 5 and conclude in section 6.

2. Background. In this section, we first set up the Bayesian inverse problem and review how it is solved using the standard Metropolis-Hastings MCMC (MH-MCMC) algorithm. We then focus on the multi-fidelity methods and introduce the ACV and MLMC frameworks for variance reduction.

2.1. Bayesian inverse Problems and MCMC. Let (X, \mathcal{X}) , with $X \subseteq \mathbb{R}^d$, be a measurable space, and define the forward model for the Bayesian inverse problem (BIP) as $\mathcal{F} : \theta \rightarrow \mathbb{R}$. Here, $\theta \in X$ is the set of parameters controlling the model output. Assuming an additive error model, the model is expressed as $y = \mathcal{F}(\theta) + \epsilon$ where $\epsilon \sim \mathcal{N}(0, \Sigma)$ is the Gaussian noise with covariance Σ .

Given observations $y_{\mathcal{D}} \in \mathbb{R}$ of the model, the BIP seeks a posterior distribution of the parameter set θ denoted by $\pi(\theta)$. This posterior distribution is given by Bayes rule when assuming a prior $\pi^0(\theta)$:

$$(2.1) \quad \pi(\theta) = \frac{\mathcal{L}(\theta)\pi^0(\theta)}{Z},$$

where

$$(2.2) \quad \mathcal{L}(\theta) = \frac{1}{\sqrt{2\pi}^d \sqrt{|\Sigma|}} \exp\left(-\frac{1}{2} (y_{\mathcal{D}} - \mathcal{F}(\theta))^T \Sigma^{-1} (y_{\mathcal{D}} - \mathcal{F}(\theta))\right),$$

is the likelihood under Gaussian noise and Z is the normalizing constant.

The posterior has no closed form solution for general cases, and sampling approaches based on MCMC are used to generate samples distributed according to π . MCMC approaches create a sequence of random variables $\{\theta^i\}_{i=1}^N$, where θ^i is the state of the chain at iteration i and the stationary distribution is the posterior $\pi(\theta)$. Among these methods, the MH-MCMC algorithm [16] is the most popular and widely used. The proposal distribution $q(\cdot, \cdot)$ and the acceptance probability $\alpha(\cdot, \cdot)$ define the algorithm. Samples are proposed iteratively using q and are accepted or rejected based on α . The algorithm is shown in Algorithm 2.1 and induces a Markov transition kernel of the form:

$$(2.3) \quad K(\theta, A) = \int_A \alpha(\theta, \theta^*) q(\theta, d\theta^*) + \left(\int_X 1 - \alpha(\theta, \theta^*) q(\theta, d\theta^*) \right) \delta_{\theta}(A), \quad A \in \mathcal{X},$$

where δ is the Dirac delta function. Existence of a stationary distribution is guaranteed if the kernel (2.3) satisfies detailed balance, and convergence is guaranteed if the kernel is ergodic. Further proof and reading can be found in [16, 32]. Given the abil-

Algorithm 2.1 Metropolis-Hastings MCMC [16]

- 1: **Input:** π, N, q, θ^0
- 2: **for** $i = 0, 1, \dots, N - 1$ **do**
- 3: Sample θ^* from $q(\theta^i, \cdot)$
- 4: Sample $u \sim \mathcal{U}(0, 1)$
- 5: Set $\theta^{i+1} = \theta^*$ if $u < \alpha$ where

$$\alpha(\theta^i, \theta^*) = \min\left(1, \frac{\pi(\theta^*) q(\theta^i, \theta^*)}{\pi(\theta^i) q(\theta^*, \theta^i)}\right),$$

- 6: Set $\theta^{i+1} = \theta^i$ otherwise
 - 7: **end for**
 - 8: **return** $\{\theta^i\}_{i=1}^N$
-

ity to sample from the posterior $\pi(\theta)$, we are interested in making model predictions by computing statistics of some quantity of interest Q . For example, a Monte Carlo estimator for the expectation is

$$(2.4) \quad \hat{Q} = \mathbb{E}_{\theta \sim \pi}[Q] = \int_{\theta \in \Theta} Q(\theta) \pi(\theta) d\theta \approx \frac{1}{N} \sum_{i=1}^N Q(\theta^i), \quad \theta^i \sim \pi,$$

where the notation \hat{Q} denotes an estimator for the mean of Q obtained by generating N samples $\{\theta^i\}_{i=1}^N$ from the distribution π . The first equality in (2.4) comes from writing the estimate of the mean as an expectation, the second equality comes from writing the expectation as an integral and the approximation comes from writing the integral as a Monte Carlo estimation with N samples.

The estimator in (2.4) is unbiased with respect to the model used. The error of this estimator is measured by its variance, and when the variance of Q is finite, the variance of the estimator is inversely proportional to the number of samples N . In this paper, we do not consider the bias of the model with respect to representing some underlying truth model, and therefore our goal is to reduce the error of this procedure through variance reduction. Here, we employ multi-fidelity techniques.

2.2. Control variates and multi-fidelity models. The Monte Carlo estimator in (2.4) is computationally expensive, with improvements to accuracy requiring orders of magnitude more samples. One strategy to address this challenge is to leverage multi-fidelity techniques that combine estimates from an ensemble of models to achieve a significantly lower variance. This ensemble typically includes a high-fidelity model and several low-fidelity models. In the context of a discretized PDE parameterized by the discretization parameter ℓ , the low fidelity models are coarse grid approximations of the original discretization given by $\{\mathcal{F}_\ell\}_{\ell=0}^L$. Similarly, we obtain a hierarchy of output functionals $\{Q_\ell\}_{\ell=0}^L$. In the following, outputs with subscript L are assumed to be the highest fidelity with respect to which we seek variance reduction.

Although a plethora of multi-fidelity techniques have been explored in the past [29], in this work, we will focus on creating *fusion* estimators of the type,

$$(2.5) \quad \hat{Q}_L^{\text{MF}} = f\left(\hat{Q}_0, \hat{Q}_1, \dots, \hat{Q}_L\right),$$

where \hat{Q}_ℓ denotes the estimator of the quantity of interest at levels $\ell = 0, 1, \dots, L$ and $f(\cdot)$ is a function that combines these estimators. The goal of the fusion estimator is to reduce the variance of the estimator \hat{Q}_L^{MF} by exploiting the correlation between the estimators \hat{Q}_ℓ at different levels. Both the choice of the function $f(\cdot)$ and the correlation between the multi-fidelity estimators play a crucial role in determining the efficiency of the estimator.

2.2.1. Control variate estimator. The CV is a classical approach for linear information fusion. This method exploits *known* expectations of the lower fidelity models $\{\mu_\ell\}_{\ell=0}^{L-1}$ and their correlations to the output to obtain an estimator with reduced variance according to

$$(2.6) \quad \hat{Q}_L^{\text{CV}} = \hat{Q}_L + \sum_{\ell=0}^{L-1} \beta_\ell \left(\hat{Q}_\ell - \mu_\ell\right),$$

for some control variate weight vector $\beta = (\beta_0, \beta_1, \dots, \beta_{L-1})$. The estimator in (2.6) is clearly unbiased and the variance of the estimator is dependent on the correlation between the level dependent control variates Q_0, Q_1, \dots, Q_L and the control variate weight β . For a given covariance structure, the weights β can be optimized to minimize the variance of the CV estimator [24]. The key point is that, the greater the correlation between the control variates and the functional quantity, the lower the variance of the CV estimator.

2.2.2. Approximate control variate estimators. In practice, the means $\{\mu_\ell\}_{\ell=0}^{L-1}$ are unknown and have to be estimated from lower fidelities. This leads to the approximate control variate (ACV) estimator [13] given by:

$$(2.7) \quad \hat{Q}_L^{\text{ACV}} = \hat{Q}_L + \sum_{\ell=0}^{L-1} \beta_\ell \left(\hat{Q}_\ell - \hat{\mu}_\ell\right),$$

with $\hat{\mu}_\ell$ the estimated mean of the control variate Q_ℓ at level ℓ . The ACV estimator is unbiased and the variance of the estimator is dependent on the correlation between the highest fidelity functional estimator \hat{Q}_L and the difference terms $\{\hat{Q}_\ell - \hat{\mu}_\ell\}_{\ell=0}^{L-1}$ (Proposition 2 in [13]). Similar to the CV estimator, the key is to maximize the correlation between the difference terms and the functional quantity.

If the control variate weights in (2.7) are each set to $\beta_\ell = -1$, we end up with the Multilevel Monte Carlo [12] framework by rewriting the estimator as a telescoping sum:

$$(2.8) \quad \hat{Q}_L^{\text{MLMC}} = \hat{Q}_0 + \sum_{\ell=1}^L \hat{Q}_\ell - \hat{Q}_{\ell-1} = \sum_{\ell=0}^L \hat{Y}_\ell,$$

where the level wise estimator is defined as $\hat{Y}_\ell = \hat{Q}_\ell - \hat{Q}_{\ell-1}$ and $\hat{Y}_0 = \hat{Q}_0$. As opposed to ACV where there is potential to couple all the level dependent functionals, MLMC simplifies the estimation procedure by only coupling successive levels. The MLMC estimator is unbiased and the variance of the estimator is dependent on the variance of each of the terms $\{\hat{Y}_\ell\}_{\ell=0}^L$ on the right-hand side of (2.8). The key is then to create highly correlated estimators \hat{Q}_ℓ and $\hat{Q}_{\ell-1}$ by coupling samples that will result in $\mathbb{V}[\hat{Y}_\ell] \rightarrow 0$ as $\ell \rightarrow \infty$. Consider the variance of the level wise estimator at a particular level ℓ given by:

$$\mathbb{V}[\hat{Y}_\ell] = \mathbb{V}[\hat{Q}_\ell] + \mathbb{V}[\hat{Q}_{\ell-1}] - 2\text{Cov}[\hat{Q}_\ell, \hat{Q}_{\ell-1}].$$

Assuming $\mathbb{V}[\hat{Q}_\ell] \approx \mathbb{V}[\hat{Q}_{\ell-1}] = V$ and using the Pearson correlation coefficient,

$$\rho_\ell = \text{Cov}[\hat{Q}_\ell, \hat{Q}_{\ell-1}] / \sqrt{\mathbb{V}[\hat{Q}_\ell]\mathbb{V}[\hat{Q}_{\ell-1}]},$$

we can write the variance as:

$$\mathbb{V}[\hat{Y}_\ell] = 2V(1 - \rho_\ell).$$

We can clearly see how the variance of the MLMC estimator can be reduced by increasing the correlation between the level dependent functional estimators. In standard MLMC applications, when exact sampling is possible for the forward problem, this can be easily achieved by sharing samples for both the fine and coarse estimators at a particular level. This technique is particularly evident in Stochastic Differential Equations [12] and hyperbolic PDE's [6]. However, for inverse problems, the distributions of each level may be different and correspond to the inverse problem at each such level.

3. Inverse problem estimators and couplings. In the inverse case, where MCMC sampling is employed, achieving high correlations between the functional estimators becomes significantly complex. The dependency on the forward model introduced by MCMC methods complicates direct sharing of samples, *making it challenging to use the same input samples for each level, as is typical for ACV approaches for forward problems*. These challenges necessitate studying *couplings* that can efficiently establish and exploit such correlations within the MCMC framework. In this section, we will formally introduce couplings and demonstrate their critical role in variance reduction. Then, we will extend our discussion to the integration of ACV and MLMC frameworks with MCMC methods to reduce the computational cost of the estimation procedure for inverse problems.

3.1. Couplings. Let (X, \mathcal{X}, μ) and (Y, \mathcal{Y}, ν) be two probability spaces. Coupling of two probability measures μ and ν is defined as a joint probability measure Γ on $(\Omega, \mathcal{O}, \Gamma)$ where $\Omega = X \times Y$ and $\mathcal{O} = \mathcal{X} \otimes \mathcal{Y}$, such that the marginals of Γ are μ and ν [35]. In other words, for all measurable sets $A \in \mathcal{X}$ and $B \in \mathcal{Y}$, we have $\Gamma[A \times Y] = \mu(A)$ and $\Gamma[X \times B] = \nu(B)$. Couplings are usually used to establish some distributional properties between the two measures μ and ν . For instance, they can be employed to analyze the distance between probability measures in terms of distance metrics [34], to facilitate transportation problems [35], or to prove convergence properties of MCMC methods [2, 26]. More recently, novel couplings have been proposed to exploit variance reduction and provide unbiased estimations [19, 18] in the context of MCMC.

Couplings can be broadly classified into two categories: *deterministic* and *non-deterministic* [35]. In deterministic couplings, the relationship between two random variables X and Y defined on the two probability spaces can be described by a function. Formally, this translates to the existence of a measurable function $T : X \rightarrow Y$ such that $Y = T(X)$. An important deterministic coupling example is the optimal transport (OT) problem which aims to find the optimal transport map by introducing a cost function $c(x, y)$ on Ω that can be interpreted as the work needed to transport a unit of mass from x to y . Some applications of OT can be found in [28, 27]. Non-deterministic couplings, referred to simply as couplings, arise from invoking randomization during their construction and are described through a joint probability measure Γ on Ω . A notable example is the maximal coupling technique [34], where the joint distribution Γ is constructed such that the probability of the random variables X and Y being equal is maximized [34].

We now extend the concept of coupling to Markov chains in the following way [34, 26]: suppose we have an ergodic MCMC kernel $K_X : X \times \mathcal{X} \rightarrow [0, 1]$ with measure μ and another ergodic MCMC kernel $K_Y : Y \times \mathcal{Y} \rightarrow [0, 1]$ with measure ν . A coupling of these two chains is a joint Markov kernel $K : \Omega \times \mathcal{O} \rightarrow [0, 1]$ with joint measure Γ satisfying the following property:

$$\begin{aligned} \int_{\mathcal{Y}} K((x, y), A \times dy) &= K_X(x, A), \\ \int_{\mathcal{X}} K((x, y), dx \times B) &= K_Y(y, B). \end{aligned}$$

These equations imply that the marginals of the joint kernel K are the kernels K_X and K_Y . Also, any Markov chain $\{Z^i\}_{i=1}^N = (\{X^i\}_{i=1}^N, \{Y^i\}_{i=1}^N)$ constructed with the joint kernel K is composed such that the sequences $\{X^i\}_{i=1}^N$ and $\{Y^i\}_{i=1}^N$ follow the transition dynamics of their respective kernels K_X and K_Y . Note that the coupling kernel K is not unique and the sequences maintain a relationship with each other that depends on the specific coupling technique used.

In this work, we are dealing with MH-MCMC type methods for our inverse problem estimators, and finding a way to create efficient couplings is crucial for our purposes. The authors in [26] show how any coupling of MH-MCMC like kernels can be represented as a combination of a proposal coupling (q_X and q_Y) followed by an acceptance coupling (α_X and α_Y). Specifically, to effectively couple two Markov chains together, we first couple the proposal distributions to produce a proposed state $Z^* = \{X^*, Y^*\}$ given the current state $Z^i = \{X^i, Y^i\}$. We then perform the acceptance coupling step by marginally accepting or rejecting the proposed state on both chains using the same uniform random number in the accept-reject function (step 5 in Algorithm 2.1). This insight provides a structured approach to construct efficient

couplings for MH-MCMC type kernels, emphasizing the need for efficient proposal couplings.

3.2. Multilevel Markov chain Monte Carlo (ML-MCMC) estimators.

We are now in a position to discuss how the ACV frameworks can be integrated with MCMC methods to reduce the computational cost of the estimation procedure for inverse problems. In this work, we focus on the ML-MCMC framework and illustrate how the coupling techniques discussed in subsection 3.1 can be used to construct coupled Markov chain samples $\theta_{\ell, \ell-1}^i = \{\theta_\ell^i, \theta_{\ell-1}^i\} \sim \Gamma_\ell^i$. ACV-MCMC schemes can be constructed similarly and will be subject to future work. Consider the MLMC estimator (2.8) specialized to the Monte Carlo estimate case

$$(3.1) \quad \hat{Q}^{\text{ML-MCMC}} = \frac{1}{N_0} \sum_{i=1}^{N_0} Q_0(\theta_0^i) + \sum_{\ell=1}^L \frac{1}{N_\ell} \sum_{i=1}^{N_\ell} (Q_\ell(\theta_\ell^i) - Q_{\ell-1}(\theta_{\ell-1}^i)),$$

assuming that the Markov chains are sufficiently burned in.

For the ML-MCMC estimator (3.1) to be unbiased, we can either ensure that all Markov chains share a common target distribution $\{\Theta_0^i, \Theta_1^i, \dots, \Theta_L^i\} \sim \pi_L$, or that each chain follows its respective level-dependent target distribution $\Theta_0^i \sim \pi_0, \Theta_1^i \sim \pi_1, \dots, \Theta_L^i \sim \pi_L$. In the first case, if we set the target distribution to be the highest fidelity posterior π_L , analogous to standard MLMC, the cost on all levels would be dominated by the evaluation of the likelihood on the finest level. This would negate any potential cost reduction benefits offered by sharing the samples. Conversely, the second case is more practical, wherein the chains are sampled from a coupled kernel whose marginals correspond to the level-dependent posteriors.

To maximize the correlation between the last two quantities in (3.1), we can leverage the coupling framework to construct an optimal joint distribution at each level of the estimator. This reduces the problem to constructing efficient proposal couplings ($\Gamma_\ell = \{q_\ell, q_{\ell-1}\}$) of the level dependent Markov chains as discussed in subsection 3.1. Achieving efficient proposal couplings facilitates high correlations between the chains, essential for reducing the variance of the level wise (difference) estimators in (3.1). Once the coupling is established, we can solve an optimization problem [12] to find the optimal number of samples for each level depending on the covariance structure of the functional estimates.

We now provide a meta-algorithm for the ML-MCMC framework in Algorithm 3.1. The first step in the base algorithm is to sample from the lowest fidelity posterior distribution π_0 using any ergodic MCMC algorithm, for example, Algorithm 2.1. Then, for the successive levels, based on the coupling method for the joint distribution, we construct a coupled Markov chain $\{\Theta_\ell^i, \Theta_{\ell-1}^i\}$ for which the marginal chains at two successive levels are highly correlated but at the same time, sampled from their respective marginal distributions. This is done by proposing a joint state from the coupled Markov kernel followed by an accept-reject step based on the same uniform random number u as discussed in subsection 3.1. The probability density function (pdf) of the proposal distribution used in proposing the joint state is also returned from each coupling method to be used in the level wise accept-reject step. The coupled chains along with the coarsest level chain are saved and returned. The samples from all the chains are then used to compute the functional quantities used in the estimator.

3.3. Existing coupling methods for ML-MCMC. In this section, we will review some existing non-deterministic coupling methodologies that couple the MCMC chains in the ML-MCMC framework.

Algorithm 3.1 Meta algorithm for multilevel Markov chain Monte Carlo

```

1: Input:  $\{\pi_\ell, N_\ell, \theta_\ell^0\}_{\ell=0}^L, q_0, \text{Coupling-Method}$ 
2: if  $\ell = 0$  then
3:    $\{\theta_0^i\}_{i=1}^{N_0} = \text{MH-MCMC}(\pi_0, N_0, q_0, \theta_0^0)$ 
4:   Save the chain  $\Theta_0^i = \{\theta_0^i\}_{i=1}^{N_0}$ 
5: end if
6: for  $\ell = 1, 2, \dots, L$  do
7:   Sample  $\theta_{\ell-1}^0$  from  $\{\theta_{\ell-1}^i\}_{i=1}^{N_0}$  or use input
8:   for  $i = 0, 1, \dots, N_\ell - 1$  do
9:      $\{\theta_\ell^*, \theta_{\ell-1}^*\}, \{q_\ell, q_{\ell-1}\} = \text{Coupling-Method}(\{\pi_\ell, \pi_{\ell-1}\}, \{\theta_\ell^i, \theta_{\ell-1}^i\})$ 
10:    Sample  $u \sim \mathcal{U}(0, 1)$ 
11:    for  $j = \ell; \ell - 1$  do
12:      Set  $\theta_j^{i+1} = \theta_j^*$  if  $u < \alpha_j$ , where

```

$$\alpha_j(\theta_j^i, \theta_j^*) = \min \left(1, \frac{\pi_j(\theta_j^*)q_j(\theta_j^*, \theta_j^i)}{\pi_j(\theta_j^i)q_j(\theta_j^i, \theta_j^*)} \right)$$

```

13:      Set  $\theta_j^{i+1} = \theta_j^i$  otherwise
14:    end for
15:  end for
16:  Save the coupled chains  $\Theta_{\ell, \ell-1}^i = \{\theta_\ell^i, \theta_{\ell-1}^i\}_{i=1}^{N_\ell}$ 
17: end for
18: return  $\left( \Theta_0^i, \left\{ \Theta_{\ell, \ell-1}^i \right\}_{\ell=1}^L \right)$ 

```

3.3.1. Coarse Proposal. The first method is inspired by [5] where the authors state that since the posterior distributions π_ℓ and $\pi_{\ell-1}$ are both approximations of the true posterior π , the samples from π_ℓ will be very similar to the samples from $\pi_{\ell-1}$. *This leads to the idea that one can use the samples from the coarse level posterior distribution $\pi_{\ell-1}$ as a proposal for the fine level posterior distribution π_ℓ .* Only if the coarse level proposal is accepted, the fine level accept or reject step is performed. This method requires less computational effort compared to the standard MCMC method because the fine level forward model is called only if the coarse level proposal is accepted.

In [7], the authors employ this two step procedure to the ML-MCMC framework by trying to produce an independent sample from the coarse level posterior distribution as a proposal for the fine level chain by recursive sub-sampling. The algorithm is shown in Algorithm 3.2. The major drawback with this method is that one cannot produce an independent sample from the coarse level posterior distribution and hence the coupled chains cannot be proved to be ergodic, incurring an inherent bias in the estimation procedure [7, 23]. In [21], the authors extend the idea of [7] by coupling successive levels of the ML-MCMC chain using recursivity. This eliminates the need to subsample from the coarse level posterior distribution and hence does not introduce bias in the estimation procedure. However, this causes a factorial increase in the computational cost as the number of levels increase.

Another apparent disadvantage is with the initial assumption of the posterior distributions being close to each other which is not always the case in practice. This

Algorithm 3.2 Coupling-Method: Coarse Proposal [7, 21]

- 1: **Input:** $\{\pi_\ell, \pi_{\ell-1}\}, \{\theta_\ell^i, \theta_{\ell-1}^i\}$
 - 2: Produce an independent sample $\theta^* \sim \pi_{\ell-1}$
 - 3: Set $\theta_{\ell-1}^*, \theta_\ell^* = \theta^*$
 - 4: Set $q_\ell = \pi_{\ell-1}$
 - 5: **return** $\{\theta_\ell^*, \theta_{\ell-1}^*\}, \{q_\ell, q_{\ell-1}\}$
-

creates proposals that are not accepted which leads to bad mixing and additional computational burden while imposing strict restrictions on the choice of the low fidelity approximation that we intend to circumvent.

3.3.2. Independent Proposal. The next method couples the two chains in (3.1) via independent Metropolis-Hastings type proposals. The authors in [23] *couple the two chains with a proposal that is independent of the current state of either chain followed by an accept-reject step based on the same uniform random number*. This approach ensures the generation of marginally true chains that are correlated, assuming the chains exhibit a good overall acceptance rate and demonstrate effective mixing. They also show that under some conditions on the proposal and posterior densities, there exists a unique invariant probability measure for the coupled chain. An important restrictive assumption (A.1. in [23]) which states that the tails of the proposal distribution should decay more slowly than the tails of the posterior distribution of the coupled chains is required for the coupled chains to be ergodic.

Algorithm 3.3 Coupling-Method: Independent Proposal [23]

- 1: **Input:** $\{\pi_\ell, \pi_{\ell-1}\}, \{\theta_\ell^i, \theta_{\ell-1}^i\}$
 - 2: Construct independent proposal $q_\ell^*(\mu_\ell^{\text{IMH}}, \Sigma_\ell^{\text{IMH}})$
 - 3: Sample $\theta^* \sim q_\ell^*(\cdot, \cdot)$ from the independent proposal
 - 4: Set $\theta_{\ell-1}^*, \theta_\ell^* = \theta^*$
 - 5: Set $q_{\ell-1}, q_\ell = q_\ell^*(\cdot, \cdot)$
 - 6: **return** $\{\theta_\ell^*, \theta_{\ell-1}^*\}, \{q_\ell, q_{\ell-1}\}$
-

This restrictive assumption on the proposal is a major drawback for the coarse level proposal methods discussed in subsection 3.3.1. The authors in [23] clearly show that the coupled chain in coarse level proposal methods will not be ergodic unless the proposal distribution satisfies the condition in A.1., which is usually the case in practice. However, the independent proposal method has its own challenges, particularly in selecting an appropriate proposal distribution that satisfies the tail decay assumption while maintaining sufficient correlation between the chains. Given that the posterior distributions of the coupled chains are unknown, determining a suitable proposal distribution for the tail decay assumption becomes a non-trivial task. The authors in [23] recommend utilizing density approximation techniques such as Kernel Density Estimation (KDE), flow-based generative models, or Laplace Approximations of the posterior distributions as viable proposal candidates. Nevertheless, these methods introduce additional computational complexity to the problem.

3.3.3. Maximal Coupling. The concept of maximal coupling has been primarily used to prove convergence properties of MCMC chains [34]. A maximal coupling between two distributions π_ℓ and $\pi_{\ell-1}$ is a distribution of random variables $\{\Theta_\ell, \Theta_{\ell-1}\}$

that maximizes $\mathbb{P}(\Theta_\ell = \Theta_{\ell-1})$ while satisfying $\Theta_\ell \sim \pi_\ell$ and $\Theta_{\ell-1} \sim \pi_{\ell-1}$. The authors in [19] use this idea of maximal coupling to eliminate the burn-in bias in MCMC. They do so by coupling proposals for two chains with the same inherent target distribution. The author in [22] expands on this idea by *maximally coupling chains at successive levels in the ML-MCMC framework. This is done by sampling $\{\theta_\ell^{i+1}, \theta_{\ell-1}^{i+1}\}$ from a maximal coupling of $\Gamma_\ell = \{q_\ell, q_{\ell-1}\}$ such that $\theta_\ell^{i+1} \sim q_\ell(\theta_\ell^i, \cdot)$ and $\theta_{\ell-1}^{i+1} \sim q_{\ell-1}(\theta_{\ell-1}^i, \cdot)$, with $\mathbb{P}(\theta_\ell^{i+1} \neq \theta_{\ell-1}^{i+1}) = \|q_\ell(\theta_\ell^i, \cdot) - q_{\ell-1}(\theta_{\ell-1}^i, \cdot)\|_{tv}$, where $\|\cdot\|_{tv}$ is the total variation distance.*

Note that even though we term this method as a maximal coupling of the two chains, the proposal distributions are coupled and a subsequent accept-reject step is performed with a common uniform random number. A procedure to sample from such a maximal coupling is taken from [34] called the γ -coupling. The readers are referred to [19, 26] for more such sampling techniques to sample from maximally coupled kernels. The algorithm for the maximal coupling is given in Algorithm 3.4.

Algorithm 3.4 Coupling-Method: Maximal Coupling [22]

- 1: **Input:** $\{\pi_\ell, \pi_{\ell-1}\}, \{\theta_\ell^i, \theta_{\ell-1}^i\}, \Gamma_\ell(\cdot, \cdot)$
 - 2: Sample $\{\theta_\ell^*, \theta_{\ell-1}^*\} \sim \Gamma_\ell(\theta_\ell^i, \theta_{\ell-1}^i)$ (Algorithm 2 in [19])
 - 3: **return** $\{\theta_\ell^*, \theta_{\ell-1}^*\}, \{q_\ell, q_{\ell-1}\}$
-

Although this method allows for state-dependent proposals in contrast to the independent proposal method, and is relatively inexpensive to implement, the correlation between the chains depends on the total variation distance between the two proposal distributions, with smaller distances being preferable. Since the proposals are state-dependent, it is desirable for samples to be close to each other. However, achieving this proximity is not always feasible for high dimensions or when the posterior distributions differ, as is often the case in practice.

4. Proposed coupling methodology. In this section, we propose a new algorithm termed as the SYNchronized step Correlation Enhancement (SYNCE) coupling to couple the level wise chains in the ML-MCMC estimator. We discuss the advantages of the proposed method compared to the existing algorithms and provide a detailed framework for the same.

4.1. Synchronized step correlation enhancement. Our proposed method is inspired from [31], where the authors coupled two Markov chains by using the idea of common random numbers. They coupled the chains of the true distribution and a Gaussian approximation of the true distribution to reduce the variance of their estimator. The authors state that *two chains are coupled when their transitions are determined by the same random numbers*. We extend this idea to our framework by using common random numbers for the two chains that sample from the ℓ 'th and $(\ell - 1)$ 'th level posterior distributions. The first random number $\eta \sim \mathcal{N}(0, C)$ will be used as the covariance of the proposal distribution for both the levels and the second random number is the common uniform random number $u \sim \mathcal{U}(0, 1)$ for the accept-reject step. Note that the idea of using the common uniform random number can be found in the independent proposal and maximal coupling methods as well. Using the same random numbers η and u for both the chains ensures that the two chains are coupled and that the samples from the two chains are highly correlated. The *simplest* form of our proposed approach is given in Algorithm 4.1.

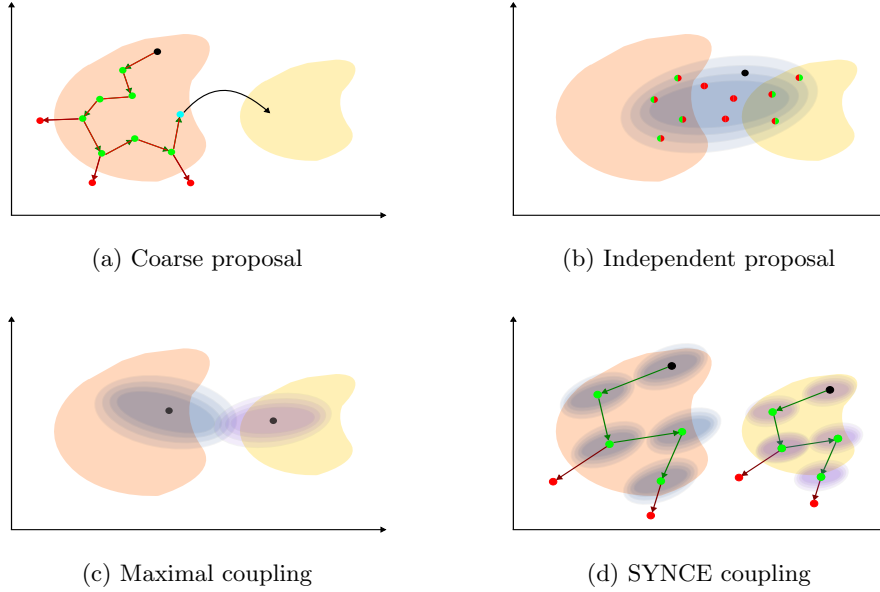


Fig. 1: Comparison of the four coupling methods for two posteriors at levels $\hat{\ell}-1$ and $\hat{\ell}$ that are substantially different. The black dot is the starting point of the chain, the green dots with the green arrows are accepted proposals and the red dots with the red arrows are rejected proposals.

Figure 1a: After the coarse chain is run for some time, the last accepted point is used as a proposal for the fine chain. We can see that most of the proposals will be rejected leading to bad mixing and low correlation.

Figure 1b: A common sample is proposed from the independent proposal distribution for both the chains. The sample is either rejected by both chains (all red), accepted by both chains (all green) or accepted by one chain and rejected by the other (green and red).

Figure 1c: The proposals are coupled using a maximal coupling kernel. The kernel tries to sample a common point from the overlapping region of the two proposal distributions. Even if we do sample, both the chains will reject the proposal.

Figure 1d: The SYNCE coupling method couples the chains by forcing the proposals to have the same magnitude and direction of change. The proposals are either accepted or rejected by their respective posteriors.

Algorithm 4.1 Coupling Method: SYNCE Coupling

- 1: **Input:** $\{\pi_\ell, \pi_{\ell-1}\}, \{\theta_\ell^i, \theta_{\ell-1}^i\}, C_\ell$
 - 2: Sample $\eta \sim \mathcal{N}(0, C_\ell)$
 - 3: Set $\theta_\ell^* = \theta_\ell^i + \eta$ and $\theta_{\ell-1}^* = \theta_{\ell-1}^i + \eta$
 - 4: Set $q_{\ell-1} = \mathcal{N}(\theta_{\ell-1}^i, C_\ell)$ and $q_\ell = \mathcal{N}(\theta_\ell^i, C_\ell)$
 - 5: **return** $\{\theta_\ell^*, \theta_{\ell-1}^*\}, \{q_\ell, q_{\ell-1}\}$
-

The proposed coupling method offers significant advantages compared to the other

Method	Pros	Cons
Coarse proposal [7, 21]	Good when posteriors are close	Bad mixing, factorial cost and non-ergodic
Independent proposal [23]	Good correlation and ergodic	Constructing the independent proposal
Maximal coupling [22]	Cheap and easy to implement	Requires close posteriors
SYNCE coupling [this paper]	High correlation, cheap and easy to implement	Requires tuning the common RV

Table 1: Advantages and disadvantages of all the methods discussed.

methods because it requires no assumptions about the posterior distributions, inherently satisfying the tail decay assumption by utilizing a random walk proposal centered at the previous state for each chain. Additionally, this method is highly cost-effective, involving only the generation of two random numbers. In contrast, the other three methods discussed in subsections 3.3.1 to 3.3.3 rely on the similarity of the posteriors, attempting to couple the chains using proposals that enforce the acceptance of the same sample. In Figure 1, we see how these approaches behave poorly when the posteriors are substantially different. The SYNCE method, however, correlates the samples by compelling them to have identical magnitudes and directions of change instead of forcing them to accept the same sample. When the posteriors are close, our method performs similarly if not better than the existing methods under some conditions that will be discussed in the coming sections. This approach provides a more natural and straightforward way to couple the chains, ensuring that the samples remain highly correlated. We summarize the advantages and disadvantages of the proposed method compared to the other methods in Table 1.

4.2. Ergodicity. Next we consider the ergodicity of the coupled chain induced by the proposed coupling method. We first define the Markov transition kernel for the coupled chain and then prove the ergodicity of the coupled chain. Let $K_\ell : X^2 \times \mathcal{X}^2 \rightarrow [0, 1]$ be the Markov transition kernel induced by Algorithm 4.1 and Γ_ℓ be the proposal coupling of $\{q_\ell, q_{\ell-1}\}$ at a particular MLMC level ℓ . We can use Γ_ℓ as a proposal to propose the state $\boldsymbol{\theta}_\ell^* \sim \Gamma_\ell(\boldsymbol{\theta}_\ell^i, \cdot)$ where $\boldsymbol{\theta}_\ell^* = \{\theta_\ell^*, \theta_{\ell-1}^*\}$ and $\boldsymbol{\theta}_\ell^i = \{\theta_\ell^i, \theta_{\ell-1}^i\}$. The kernel is then defined as [22]:

$$\begin{aligned}
 & K_\ell(\boldsymbol{\theta}_\ell^i, A) \\
 &= \int_{X^2} \min(\alpha_\ell(\theta_\ell^i, \theta_\ell^*), \alpha_{\ell-1}(\theta_{\ell-1}^i, \theta_{\ell-1}^*)) \Gamma_\ell(\boldsymbol{\theta}_\ell^i, d\boldsymbol{\theta}_\ell^*) \delta_{\boldsymbol{\theta}_\ell^i}(A) \\
 &+ \int_{X^2} (\alpha_\ell(\theta_\ell^i, \theta_\ell^*) - \alpha_{\ell-1}(\theta_{\ell-1}^i, \theta_{\ell-1}^*))^+ \Gamma_\ell(\boldsymbol{\theta}_\ell^i, d\boldsymbol{\theta}_\ell^*) \delta_{\theta_\ell^*, \theta_{\ell-1}^i}(A) \\
 &+ \int_{X^2} (\alpha_{\ell-1}(\theta_{\ell-1}^i, \theta_{\ell-1}^*) - \alpha_\ell(\theta_\ell^i, \theta_\ell^*))^+ \Gamma_\ell(\boldsymbol{\theta}_\ell^i, d\boldsymbol{\theta}_\ell^*) \delta_{\theta_\ell^i, \theta_{\ell-1}^*}(A) \\
 (4.1) \quad &+ \left(1 - \int_{X^2} \max\{\alpha_\ell(\theta_\ell^i, \theta_\ell^*), \alpha_{\ell-1}(\theta_{\ell-1}^i, \theta_{\ell-1}^*)\} \Gamma_\ell(\boldsymbol{\theta}_\ell^i, d\boldsymbol{\theta}_\ell^*)\right) \delta_{\boldsymbol{\theta}_\ell^i}(A),
 \end{aligned}$$

where $x^+ = \frac{x+|x|}{2}$, $x \in \mathbb{R}$ and $\alpha_\ell, \alpha_{\ell-1}$ is computed as mentioned in Algorithm 4.1. Each of the four lines in (4.1) correspond to the four possible transitions in the coupled

chain. The first line corresponds to the case where both the chains accept their respectively proposed point, the second and third lines correspond to the cases where only one of the chains accepts their proposed points and the last line corresponds to the case when both the chains reject their proposed points.

THEOREM 4.1 (Ergodicity of the coupled chain). *The coupled Markov chain induced by the Markov transition kernel K_ℓ in (4.1) is ergodic for all $\ell \in \{0, 1, \dots, L\}$.*

Proof. To prove that the Markov transition kernel K_ℓ in (4.1) is ergodic, we need to show that the kernel is irreducible, aperiodic and reversible with respect to an invariant measure ν_ℓ , if it exists. Irreducibility and aperiodicity of the coupled chain is satisfied with the choice of the random walk proposal distributions and non-zero probability of rejection in the accept-reject step for the level wise chains as in standard MH-MCMC [16, 32]. For reversibility, we can show that the transition kernel is reversible with respect to an invariant measure ν_ℓ by showing that the detailed balance condition is satisfied. The detailed proof follows from Theorem 6.3.1 in [22]. \square

4.3. Adaptation. The performance of the algorithm is highly dependent on the choice of the random number for the covariance C_ℓ . This is similar to the challenge faced in constructing the proposal distribution in the independent proposal method in Algorithm 3.3. However, unlike the independent proposal method, we do not need to choose the mean of the proposal distribution, as the proposal is a random walk centered at the previous state, simplifying this aspect of the problem. In [21], as a means to counteract the issue of different fine and coarse posteriors, the authors use an adaptive error model to correct the likelihood of the coarse models to match the fine model. This adaptive error model along with the covariance adaptation idea in [14] has been shown to improve the performance of the coarse proposal method. While this idea will definitely improve the performance of the proposed coupling method in terms of mixing, the outstanding issue of the right choice of the covariance C_ℓ still remains.

Looking at Figure 1d, we see that when steps of high magnitude are proposed, the proposals are likely to be rejected, especially if the posteriors are different. This leads to low acceptance rates, suboptimal mixing and small effective sample sizes. On the other extreme, when the steps are too small, samples are accepted quite often and the correlation is quite high, but the chains do not explore the posterior space effectively. Hence, it is important to choose the covariance C_ℓ such that we achieve a balance between good correlation, mixing and exploration. This problem of choosing the right covariance to achieve a good balance is similar to the problem of finding the optimal proposal distribution for the MH-MCMC algorithm on which there has been plenty of literature [14, 33, 2, 9, 1]. All these papers provide a framework to adapt the proposal distribution such that optimality in the sense of some target measure is reached.

A typical update algorithm for the covariance C_ℓ is given by scaling the empirical covariance with a factor λ_ℓ . The empirical covariance and mean are updated recursively using existing samples and the scaling factor λ_ℓ is updated using a Robbins-Monro recursion formula to ensure that the acceptance rate of the chain is close to some target value α^* . The updates are given by (Algorithm 4 in [1]):

$$\begin{aligned}
 \log(\lambda_\ell^{i+1}) &= \log(\lambda_\ell^i) + \gamma^{i+1} (\alpha_\ell(\theta_\ell^i, \theta_\ell^*) - \alpha^*) \\
 \mu_\ell^{i+1} &= \mu_\ell^i + \gamma^{i+1} (\theta_\ell^{i+1} - \mu_\ell^i) \\
 \Sigma_\ell^{i+1} &= \Sigma_\ell^i + \gamma^{i+1} ((\theta_\ell^{i+1} - \mu_\ell^i)(\theta_\ell^{i+1} - \mu_\ell^i)^T - \Sigma_\ell^i),
 \end{aligned}
 \tag{4.2}$$

and finally setting $C_\ell^i = \Sigma_\ell^i$ and $\theta_\ell^* = \theta_\ell^i + \lambda_\ell^i \eta$ where $\eta \sim \mathcal{N}(0, C_\ell^i)$ as before in Algorithm 4.1. The step sizes γ^i ensure that the effect of adaptation diminishes and is generally taken to be a deterministic sequence of non-increasing numbers [1]. One typically runs this algorithm for a certain number of iterations and stops adapting, considering the samples up to that point as burn-in samples. We now have an approach to adapt the covariance, but we need to adapt the covariance for both the ℓ and $\ell - 1$ chains.

When the posteriors are different or high dimensional, the adaptation parameters λ, μ and Σ for the two chains will be quite different. This will lead to the chains taking different steps and not being correlated, but achieve good mixing properties marginally. A simple and effective way to deal with this issue is to adapt the covariance C_ℓ and $C_{\ell-1}$ for both the chains separately and simultaneously, and scale the common random number sampled from a standard normal distribution with the square root of the scaled covariance as:

$$\begin{aligned}
 (4.3) \quad & \eta \sim \mathcal{N}(0, \mathcal{I}_d) \\
 & \theta_\ell^* = \theta_\ell^i + \lambda_\ell^i \sqrt{\Sigma_\ell^i} \eta \\
 & \theta_{\ell-1}^* = \theta_{\ell-1}^i + \lambda_{\ell-1}^i \sqrt{\Sigma_{\ell-1}^i} \eta,
 \end{aligned}$$

where d is the dimension of the parameter space. This ensures that the chains are coupled, and the samples are highly correlated while exploring the posterior space effectively. This formulation has ties to the optimal transport equation for two Gaussians [35], specifically for our case, transporting the sample from the standard normal Gaussian to the level dependent marginal. For the square root of the covariance, we can use the Cholesky decomposition of the covariance matrix to ensure that the covariance is positive definite.

4.4. Resynchronization. Our SYNCE coupling method with adaptation of the covariance couples chains well that are quite different in shape and location. However, when the problem is multidimensional with great difference in the target covariances, we may encounter stages where the proposed step gets accepted by one chain and rejected by the other. This leads to the chains getting out of sync and the samples losing unnecessary correlation. This is very similar to the issue of the proposals being far off in the maximal coupling method [22]. The simplest way to counteract this issue is to resynchronize the chains by considering a weighted average of two Markov kernels [22]: the SYNCE coupling kernel K_ℓ and another kernel K_ℓ^* that proposes the same sample for both the chains, such as the independent proposal kernel or the coarse proposal kernel. The resynchronization kernel K_ℓ' is given by:

$$(4.4) \quad K_\ell' = \omega_\ell K_\ell^* + (1 - \omega_\ell) K_\ell,$$

where $\omega_\ell \in (0, 1)$ is the weight. Ideally one would set ω_ℓ to 0 for small ℓ values and increase it as ℓ increases. This ensures that when the posteriors are far off from each other, no resynchronization takes place and the chains are coupled using the SYNCE coupling kernel. When the posteriors become closer with higher levels, the chains are resynchronized using both the SYNCE coupling kernel and the resynchronization kernel. This improves upon the SYNCE method to ensure that when the chains have dissimilar acceptance ratios, they are resynchronized to maintain high correlation.

The final adaptive ML-MCMC algorithm with the proposed coupling method is given in Algorithm 4.2. The algorithm improves upon Algorithm 4.1 by adapting

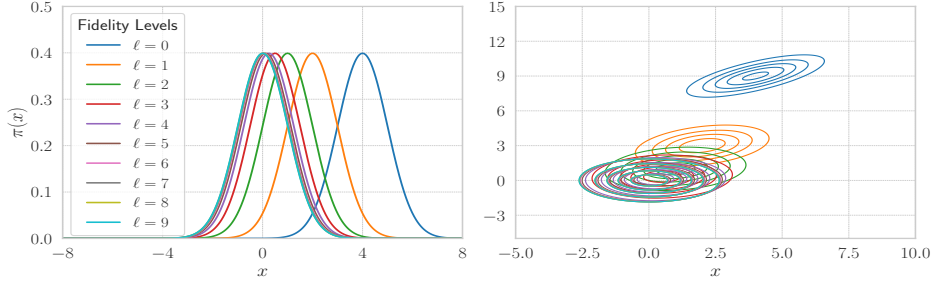


Fig. 2: Posterior distributions for the Gaussian examples at different levels. The figure on the left corresponds to subsection 5.1 and the figure on the right corresponds to subsection 5.2.

and scaling the covariance for both the chains separately and simultaneously, and resynchronizing the chains when needed for better correlation. Using resynchroniza-

Algorithm 4.2 SYNCE with adaptation and resynchronization (SYNCE-AR)

- 1: **Input:** $\{\pi_\ell, \pi_{\ell-1}\}, \{\theta_\ell^i, \theta_{\ell-1}^i\}, \{\lambda_\ell^i, \lambda_{\ell-1}^i\}, \{\Sigma_\ell^i, \Sigma_{\ell-1}^i\}, \omega_\ell$
 - 2: Sample $w \sim \mathcal{U}(0, 1)$
 - 3: Sample $\eta \sim \mathcal{N}(0, \mathcal{I}_d)$
 - 4: **if** $w \leq \omega_\ell$ **then**
 - 5: $\{\theta_\ell^*, \theta_{\ell-1}^*\}, \{q_\ell, q_{\ell-1}\} = \text{Algorithm 3.3/Algorithm 3.2}$ \triangleright resynchronize
 - 6: **else if** $w > \omega_\ell$ **then**
 - 7: Set $\theta_\ell^* = \theta_\ell^i + \lambda_\ell^i \sqrt{\Sigma_\ell^i} \eta$ and $\theta_{\ell-1}^* = \theta_{\ell-1}^i + \lambda_{\ell-1}^i \sqrt{\Sigma_{\ell-1}^i} \eta$ \triangleright SYNCE
 - 8: Set $q_{\ell-1} = \mathcal{N}(\theta_{\ell-1}^i, \Sigma_{\ell-1}^i)$ and $q_\ell = \mathcal{N}(\theta_\ell^i, \Sigma_\ell^i)$
 - 9: **end if**
 - 10: **return** $\{\theta_\ell^*, \theta_{\ell-1}^*\}, \{q_\ell, q_{\ell-1}\}$
-

tion only for the fine levels, the adaptive parameters λ, μ and Σ are used to set the mean and covariance of the independent proposal distribution in Algorithm 3.3: $\mu_\ell^{\text{IMH}} = 0.5 * (\mu_\ell^i + \mu_{\ell-1}^i)$ and $\Sigma_\ell^{\text{IMH}} = 0.5 * (\Sigma_\ell^i + \Sigma_{\ell-1}^i)$ for $\ell = 1, 2, \dots, L$. This ensures that for close and similar shaped posteriors, we obtain highly correlated chains with good mixing properties.

5. Experimental results. In this section we consider three numerical examples. To begin, we present a very simple toy problem taken from [23] to illustrate the effectiveness and sanity of the proposed methodology. The second problem is a two-dimensional extension to the first Gaussian problem that highlights the need for adaptation and resynchronization in the SYNCE coupling method. The third problem involves uncertainty quantification for Darcy flow. This example is a well known benchmark and will be used to compare the algorithms.

5.1. Shifting Gaussian. In this example, we sample from the multi-fidelity posterior distribution formed by shifting Gaussians given by $\pi_\ell = \mathcal{N}(2^{-\ell+2}, 1)$ for $\ell = 0, 1, \dots, L$. The target posteriors are plotted on the left in Figure 2. Note that this is a good example to illustrate the effectiveness of the proposed coupling method as the first two posteriors i.e, $\ell = 1$ and $\ell = 2$ are quite different (far off but similar

shaped) from each other.

In this comparison, we fix $L = 6$ and use the same Gaussian proposal $Q_\ell = \mathcal{N}(2, 3)$ across all levels for the relevant algorithms. The proposal distribution for the coarsest $\ell = 0$ level posterior is set to $Q_0 = \mathcal{N}(\cdot, 1)$ and 50,000 samples are used for all levels according to [23]. We use the same proposal covariance for the SYNCE coupling algorithm (Algorithm 4.1) with $C_\ell = 3$ to provide a fair comparison. In Figure 3, we aim to perform a sanity check if the coupling algorithms are able to sample from the right marginal distributions and demonstrate the joint distribution of certain levels for the four coupling methods.

Unlike the other three methods, we see that the coarse proposal method is unable to sample from the right marginal distributions because it breaks Assumption A1 in [23]. For the existing methods, during the sampling process, if a sample is proposed in the shared region of the posteriors, the samples get accepted by both the fine and coarse chains, creating the dominant diagonal line with slope 1 as seen in Figure 3. When the sample proposed is not inside the shared region, each chain accepts or rejects according to its accept ratio, creating the scatter seen above the diagonal line. For the coarser levels, most of the proposed samples get rejected, leading to the scatter plots being more spread out. The proposed method, however creates a diagonal line with a slope not necessarily equal to 1, taking advantage of the fact that the posteriors are shifted, without any prior knowledge about the target distributions.

In Figure 4, we show how well the samples are correlated between two successive levels. We plot the Pearson correlation coefficient between the samples at the ℓ 'th level and the $(\ell - 1)$ 'th level for the different coupling algorithms. We see that the coarse, independent and the maximal proposal methods produce samples that are not well correlated at the coarser levels. This is a direct consequence of the fact that the posteriors at these coarse levels are quite far off from each other. All the three methods depend on this closeness of the posteriors to produce correlated (same) samples at the two levels. However, our method does not depend on this closeness and rather tries to couple samples by making the two chains follow the same path using the same covariance of the two proposal distributions. This is why the SYNCE coupling method achieves the greatest correlation, particularly for the coarser models.

5.2. Rotating-shifting Gaussian. Next, we consider a 2D family of Gaussians to show benefits even in the case of changing covariance structure between the fidelities. The posterior densities are given by:

$$(5.1) \quad \pi_\ell = \mathcal{N} \left(\mu'_\ell = \begin{bmatrix} 2^{-\ell+2} \\ 3^{-\ell+2} \end{bmatrix}, \Sigma'_\ell = \begin{bmatrix} 2 & 2^{-\ell} \\ 2^{-\ell} & 1 \end{bmatrix} \right),$$

for $\ell = 0, 1, \dots, L$. We can clearly see from (5.1) and Figure 2 that this is a 2D extension of the subsection 5.1 problem where the posteriors are rotated in addition to being shifted.

Here, we show the importance of adaptation and resynchronization for the SYNCE coupling algorithm as discussed in subsections 4.3 and 4.4. We run two different experiments for this example with the number of levels set to $L = 6$ and the number of samples in each level set to 50,000. We discard the first 20,000 samples as burn in and apply any adaptation in this period to get a good estimate of the adaptation parameters. In the first experiment, we compare the vanilla SYNCE coupling method without adaptation and resynchronization (Algorithm 4.1) with the maximal coupling method. This is a fair comparison as the proposals in the maximal coupling method are state dependent and it was observed that the other existing methods per-

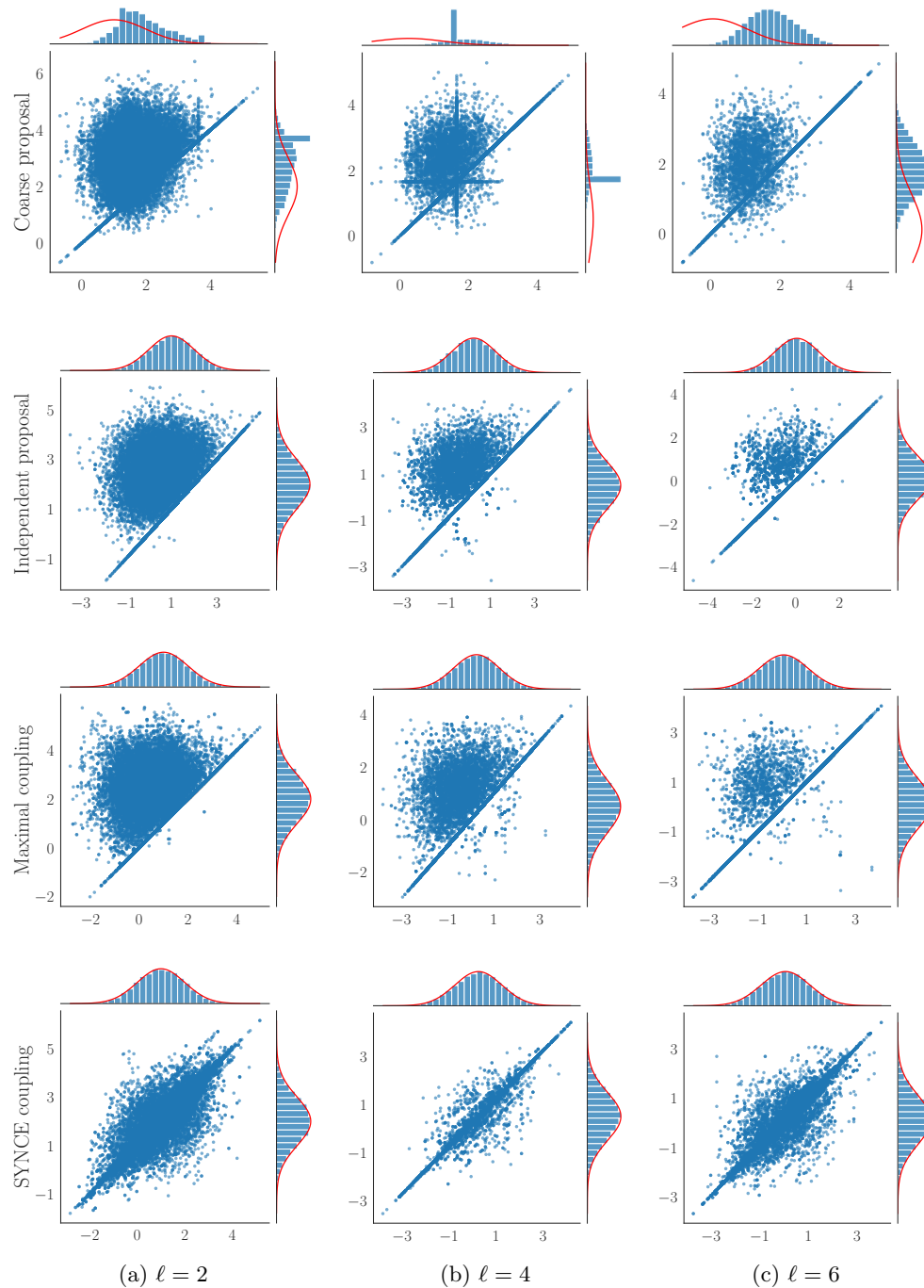


Fig. 3: Scatter plots and histograms of samples from the different coupling algorithms for the shifting Gaussian example. For each level, the X-axis represents the samples at the ℓ 'th level and the Y-axis represents the samples at the $(\ell - 1)$ 'th level. The red line on the histogram plots represents the true posterior distribution at the respective levels. Our proposed method is able to sample posterior from the right marginal distributions and create a dominant diagonal line with slope not necessarily equal to 1.

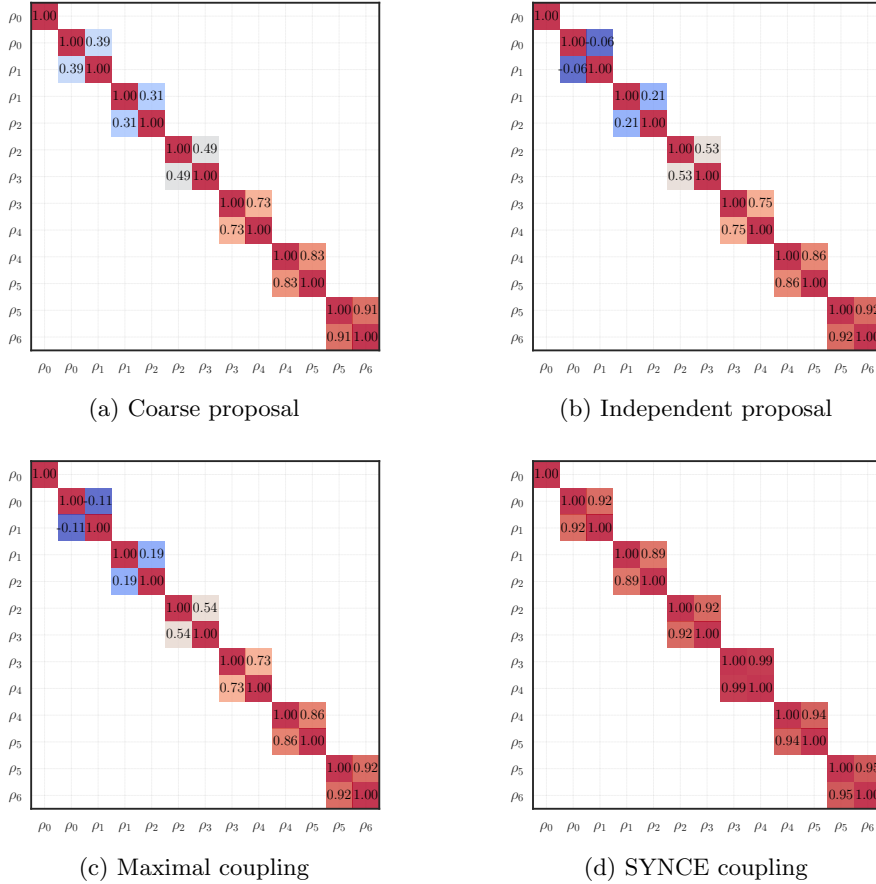


Fig. 4: Pearson correlation coefficient between samples of all levels for the shifting Gaussian example. The coefficient is a measure of how well samples are correlated. Higher correlations yield greater variance reduction and we see that the SYNCE coupling algorithm achieves the greatest correlation, particularly for the coarser models.

formed similarly. In the second experiment, we compare three algorithms: SYNCE-A, SYNCE-AR and independent proposal. SYNCE-A refers to the proposed SYNCE coupling method with only adaptation i.e, setting $\omega_\ell = 0$ for $\ell = 1, 2, \dots, L$ in Algorithm 4.2 and SYNCE-AR refers to the SYNCE coupling method with adaptation and resynchronization. This experiment highlights the importance of both scaling and resynchronizing the Markov kernel to enhance correlation in all the levels.

5.2.1. Experiment 1: SYNCE coupling vs maximal coupling. In this experiment, we set a fixed proposal distribution $Q_\ell = \mathcal{N}\left(\cdot, \begin{bmatrix} 3 & 0 \\ 0 & 3 \end{bmatrix}\right)$ for all the levels $\ell = 0, 1, \dots, L$. This proposal is chosen to ensure a 40% acceptance rate for the chains at all levels, close to the optimal value of 44% according to [9]. This choice of proposal distribution also ensures a fair comparison between the two algorithms.

In Figure 5, we plot the correlation between the samples at all levels for both

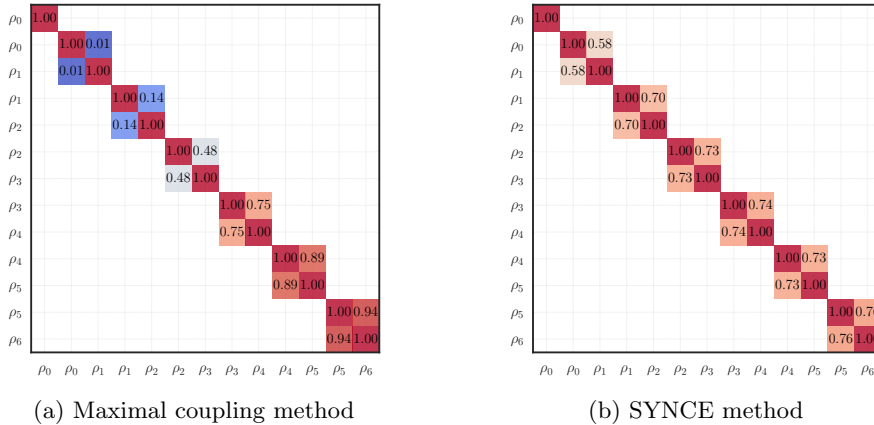


Fig. 5: Correlation plots of the sample’s first dimension, comparing the maximal coupling method to the SYNCE coupling method for the rotating-shifting Gaussian example.

the methods for the first dimension. The maximal coupling method produces samples that are highly correlated at finer levels and very poorly correlated at the coarser levels. The high distances between the posteriors at the coarse levels results in a high TV distance for the coupled kernel, leading to a low probability of a common sample being proposed for the two chains.

On the other hand, the SYNCE coupling method does produce samples that are well correlated at all levels, and, there are two important observations to be made. Firstly, there is a noticeable increasing trend in the correlation, which appears to saturate to some fixed value as we move from coarser to finer levels. At the coarsest ML-MCMC level $\ell = 1$, the correlation is significantly smaller compared to the other levels. This can be attributed to the distinct shape (covariance structure) between the two posteriors π_0 and π_1 as seen in Figure 2. Secondly, the correlation at the finest level is not as high as the maximal coupling method. Even though the posteriors are quite close in shape and distance, the two chains are not exactly in sync as the same sample is not proposed for the two chains. While taking the same step is beneficial at the coarser levels, it presents drawbacks at the finer levels. In Figure 6, we plot the autocorrelation of the samples obtained from the two methods for the finest two levels. As expected, we see that both the methods show similar decays in the autocorrelation with the same covariance of the proposal distribution. The moderate coupling at the finer levels suggest that we need modifications in our SYNCE algorithm. In the next problem, we show how adaptation and resynchronization serve this purpose.

5.2.2. Experiment 2: SYNCE-A vs SYNCE-AR vs independent proposal. In this experiment, we will compare the SYNCE coupling method with only adaptation, the SYNCE coupling method with adaptation and resynchronization, and the independent proposal coupling method. For SYNCE-A, we set the resynchronization weight $\omega_\ell = 0$ for all levels $\ell = 1, 2, \dots, L$ in Algorithm 4.2. For SYNCE-AR, we set $\omega = [0, 0, 0, 0.2, 0.3, 0.5]$ for all levels and choose the level wise independent proposal distribution $Q_\ell = \mathcal{N}\left(\mu_\ell^{\text{IMH}}, \begin{bmatrix} 3 & 0 \\ 0 & 3 \end{bmatrix}\right)$ with $\mu_\ell^{\text{IMH}} = (\mu'_\ell + \mu'_{\ell-1})/2$ as the

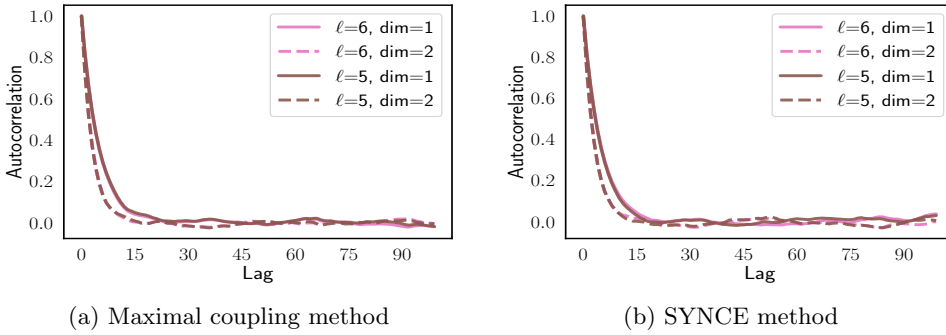


Fig. 6: Autocorrelation plots of the samples for the finest coupled level, comparing the maximal coupling method to the SYNCE coupling method for the rotating-shifting Gaussian example.

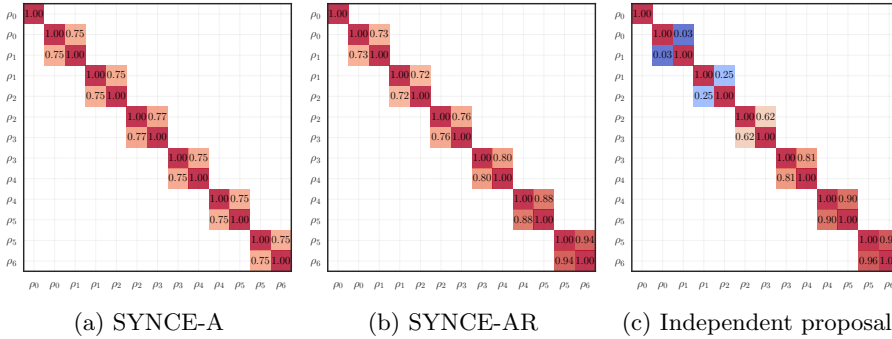


Fig. 7: Correlation plots of the sample's first dimension obtained, comparing SYNCE-A, SYNCE-AR and the Independent proposal methods for the rotating-shifting Gaussian example.

resynchronization kernel. This kernel is chosen to satisfy the tail decay assumption and to achieve optimal mixing properties for both the coupled chains. Finally, we set the target acceptance rate to 44% for all levels.

In Figure 7, we plot the correlation plots as before. We can clearly see the effect of adaptation at the coarser levels when comparing Figure 7a and Figure 5b. Rescaling each individual chain's proposal distributions to account for the respective posterior's covariance structure ensures that the chains stay in sync as much as possible while exploring the posterior space. However, at the finer levels, we are still limited by the fact that the same sample is not proposed for the two chains. This is where resynchronization comes into play. In Figure 7b, we see that introducing the resynchronization kernel promotes better syncing of the chains, especially at the finest levels where we expect the posteriors to be quite close to each other.

Finally, comparing Figure 5a, Figure 7c and Figure 7b, we see that the SYNCE coupling method with adaptation and resynchronization produces samples that are highly correlated at all levels, gaining a significant advantage over the other two

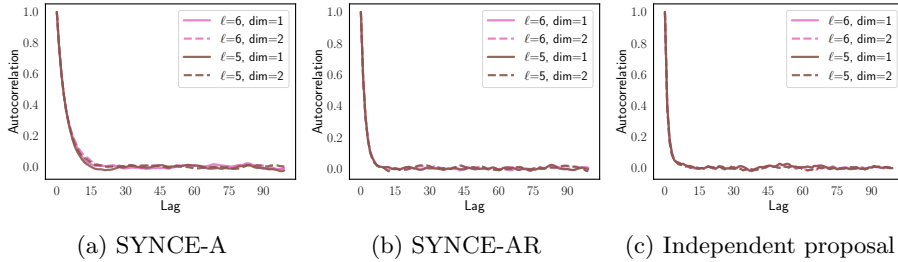


Fig. 8: Autocorrelation plots of the samples for the finest coupled level, comparing SYNCE method with only adaptation to the SYNCE method with adaptation and resynchronization for the rotating-shifting Gaussian example.

methods at the coarser levels and matching the correlation at the finer levels. In Figure 8, we plot the autocorrelation of the samples for the finest two levels. We can notice the slight improvement in the decay (Figure 8b) obtained by adapting and resynchronizing the chains as opposed to using a fixed proposal distribution.

5.3. Groundwater problem. We will now test our coupling method on the 2D Darcy’s subsurface flow equation (5.2). This is the model problem explored in great detail in [6, 7, 23] used in the uncertainty quantification of subsurface flows. The exact problem is taken from [23] and the governing equation of the problem is given by:

$$(5.2) \quad -\nabla_x \cdot (\kappa(x, \theta) \nabla_x u(x, \theta)) = 1, \quad x = (x_1, x_2) \in \Omega = [0, 1] \times [0, 1],$$

where κ represents the permeability, u represents the pressure head and $\theta \in \mathbb{R}^d, d = 4$ represents the uncertain parameters. We close the equations by providing boundary conditions on the domain as:

$$(5.3) \quad u|_{x_1=0} = 0, \quad u|_{x_1=1} = 0, \quad \partial_n u|_{x_2=0} = 0, \quad \partial_n u|_{x_2=1} = 0,$$

where ∂_n is the normal derivative with n pointing outwards from the domain. The first two conditions are the Dirichlet boundary conditions applied on the left and right boundary of the domain, and the last two conditions are the Neumann boundary conditions applied on the bottom and top boundary of the domain. The permeability field is given by [23]:

$$(5.4) \quad \kappa(x, \theta) = \exp \left(\theta_1 \cos(\pi x) + \frac{\theta_2}{2} \sin(\pi x) + \frac{\theta_3}{3} \cos(2\pi x) + \frac{\theta_4}{4} \sin(2\pi x) \right)$$

The inverse problem is to infer the uncertain parameters θ given some observed pressure head data. We generate this data by solving the forward problem (5.2) on the finest grid with a random sample of $\theta_{\text{true}} \sim \mathcal{N}(0_d, \mathcal{I}_d)$ and observing the pressure head corrupted by a Gaussian noise at 4×4 equally spaced points inside the domain. Gaussian noise is added to the observed data with a zero mean and variance $\sigma_{\text{noise}}^2 = 0.01^2$. We set the number of levels $L = 4$ and for each level ℓ , the solution of (5.2) is obtained using the Finite element method with a mesh size of $8 * 2^\ell \times 8 * 2^\ell$ triangular elements, using the FEniCS library [3].

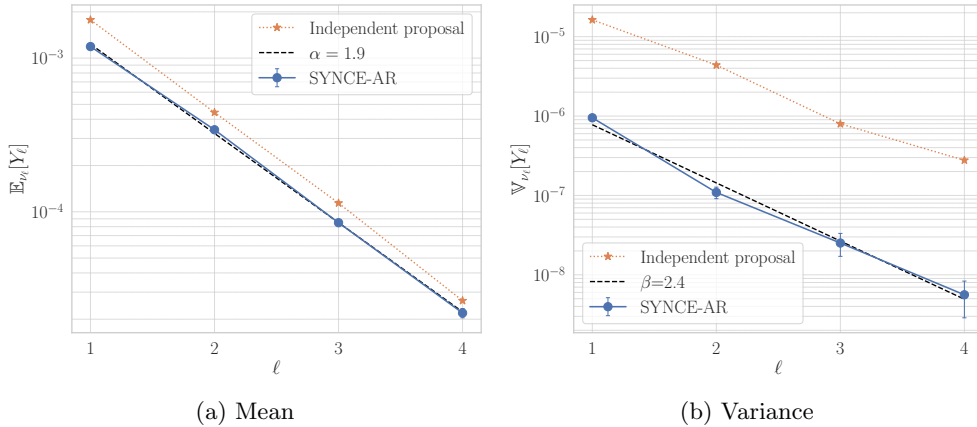


Fig. 9: Decay of error plots for the groundwater problem. The independent proposal and the SYNCE-AR methods are compared. Our method leads to almost an order or two gain in variance reduction compared to the result from [23].

The number of levels in the original problem in [23] is set to $L = 3$ with the coarsest mesh at 16×16 triangular elements. We set the number of levels to $L = 4$ with the coarsest mesh at 8×8 triangular elements as we can leverage the SYNCE coupling method to correlate samples even at very coarse levels. This is a direct consequence of the fact that the SYNCE coupling method does not depend on the closeness of the posteriors to correlate samples.

The quantity of interest (QoI) is the average pressure over the domain given by:

$$(5.5) \quad Q_\ell(\theta_\ell) = \int_{x \in \Omega} u_\ell(x, \theta_\ell) dx,$$

where Ω is the domain of the problem.

To validate the convergence rates of the proposed SYNCE coupling algorithm, we run Algorithm 3.1 with the proposed states obtained from Algorithm 4.2. We set the number of samples in each level to 10,000 and consider the first 4000 samples as burn-in. We run the algorithm for 10 independent runs and plot the decay of errors. For the coarsest chain ($\ell = 0$), we set the target acceptance ratio as 0.44 and run an adaptive MH-MCMC algorithm for that level. The two level wise adaptation parameters, the target acceptance ratio and the weight for resynchronization are set to 0.7 for each level ($\ell > 0$) and $\omega = [0.0, 0.3, 0.5, 0.7]$. These parameters were chosen to ensure low lag and high correlation between the samples at each level.

Figure 9 compares our proposed methodology to an existing result using the independent proposal method [23] for the same problem. The results for the independent proposal method were obtained by digitizing Fig. 12 in [23]. We observe that the SYNCE-AR method leads to greater variance reduction for all the level wise difference estimators Y_ℓ . Even though we use a coarser level compared to the original work, we are able to achieve almost an order or two gain in variance reduction at all levels. This is a direct consequence of the proposed coupling method that is able to correlate samples even at very coarse levels. The correlation values for the output functional at the different levels are: 0.84, 0.97, 0.99, 1.0 for $\ell = 1, 2, 3, 4$.

6. Conclusions. In this work, we presented a novel SYNCE coupling methodology for coupling Markov chains in a multilevel Markov chain Monte Carlo framework. We leverage multiple existing fidelities of computational models to construct efficient estimators that have been shown to provide significant cost reductions compared to a single fine level estimator. The performance of these estimators depend on the correlation between the samples at different levels, which in turn depends on the coupling strategy used. Opposed to existing methodologies that depend on some form of closeness between the posteriors to correlate samples, our method facilitates greater variance reduction for all levels by simply using common random numbers. The first random number is used as the covariance of the proposal distribution for the two chains at each level, and the second uniform random number is used in the accept-reject Metropolis step.

By utilizing adaptation and resynchronization, we extend our SYNCE method to adaptively rescale the proposal distributions and resynchronize the chains to enhance correlation at all levels, especially at coarse levels where the posteriors are quite different. This facilitates in using coarser levels for the estimation procedure, leading to significant computational savings. We demonstrated the effectiveness of the proposed methodology on two synthetic examples, the shifting Gaussian and the rotating-shifting Gaussian, and a real-world groundwater problem. These problems clearly show the added advantage of the proposed coupling method over the existing methods in terms of variance reduction and computational savings.

The SYNCE coupling method is the simplest realization of the proposed coupling framework we have set up. More general couplings using transport maps and non linear functions will be explored soon. Transport maps may help with mixing properties of the fine chain by learning from the coarse chain. Another possible extension to this work is to explore the use of the SYNCE coupling methodology in the context of approximate control variates. These estimators provide additional performance improvements by using a control variate weight that is estimated adaptively. Additionally, the proposed methodology can be extended in the unbiased estimation context to eliminate the burn in bias [19, 18].

REFERENCES

- [1] C. ANDRIEU AND J. THOMS, *A tutorial on adaptive MCMC*, Stat Comput, 18 (2008), pp. 343–373.
- [2] Y. F. ATCHADÉ AND J. S. ROSENTHAL, *On adaptive Markov chain Monte Carlo algorithms*, Bernoulli, 11 (2005), pp. 815 – 828.
- [3] I. A. BARATTA, J. P. DEAN, J. S. DOKKEN, M. HABERA, J. S. HALE, C. N. RICHARDSON, M. E. ROGNES, M. W. SCROGGS, N. SIME, AND G. N. WELLS, *DOLFINx: The next generation FEniCS problem solving environment*, Dec. 2023.
- [4] A. CHAUDHURI, R. LAM, AND K. WILLCOX, *Multifidelity uncertainty propagation via adaptive surrogates in coupled multidisciplinary systems*, AIAA journal, 56 (2018), pp. 235–249.
- [5] J. A. CHRISTEN AND C. FOX, *Markov chain monte carlo using an approximation*, J. Comput. Graph. Stat., 14 (2005), pp. 795–810.
- [6] K. A. CLIFFE, M. B. GILES, R. SCHEICHL, AND A. L. TECKENTRUP, *Multilevel Monte Carlo methods and applications to elliptic PDEs with random coefficients*, Comput. Visual Sci., 14 (2011), pp. 3–15.
- [7] T. J. DODWELL, C. KETELSEN, R. SCHEICHL, AND A. L. TECKENTRUP, *A hierarchical multilevel markov chain monte carlo algorithm with applications to uncertainty quantification in subsurface flow*, SIAM/ASA J. Uncertainty Quantification, 3 (2015), pp. 1075–1108.
- [8] M. EMSERMANN AND B. SIMON, *Improving simulation efficiency with quasi control variates*, Stochastic Models, 18 (2002), pp. 425–448.
- [9] A. GELMAN AND C. PASARICA, *Adaptively scaling the metropolis algorithm using expected squared jumped distance*, SSRN Journal, (2007), pp. 343–364.

- [10] G. GERACI, M. ELDRED, AND G. IACCARINO, *A multifidelity control variate approach for the multilevel monte carlo technique*, Center for Turbulence Research Annual Research Briefs, (2015), pp. 169–181.
- [11] G. GERACI, M. S. ELDRED, A. A. GORODETSKY, AND J. D. JAKEMAN, *Leveraging active directions for efficient multifidelity uncertainty quantification*, in 6th European Conference on Computational Mechanics (ECCM 6), 2018, pp. 2735–2746.
- [12] M. B. GILES, *Multilevel monte carlo methods*, Acta Numerica, 24 (2015), p. 259–328.
- [13] A. A. GORODETSKY, G. GERACI, M. S. ELDRED, AND J. D. JAKEMAN, *A generalized approximate control variate framework for multifidelity uncertainty quantification*, J. Comput. Phys., 408 (2020), p. 109257.
- [14] H. HAARIO, E. SAKSMAN, AND J. TAMMINEN, *An adaptive metropolis algorithm*, Bernoulli, 7, p. 223.
- [15] J. M. HAMMERSLEY AND D. C. HANDSCOMB, *Monte carlo methods*, in Proceedings, vol. 7, US Army Research Office., 1961, p. 17.
- [16] W. K. HASTINGS, *Monte Carlo sampling methods using Markov chains and their applications*, Biometrika, 57 (1970), pp. 97–109.
- [17] S. HEINRICH, *Multilevel monte carlo methods*, in Large-Scale Scientific Computing: Third International Conference, LSSC 2001 Sozopol, Bulgaria, June 6–10, 2001 Revised Papers 3, Springer, 2001, pp. 58–67.
- [18] J. HENG, A. JASRA, K. J. H. LAW, AND A. TARAKANOV, *On unbiased estimation for discretized models*, SIAM/ASA J. Uncertainty Quantification, 11 (2023), pp. 616–645.
- [19] P. E. JACOB, J. O’LEARY, AND Y. F. ATCHADÉ, *Unbiased Markov Chain Monte Carlo Methods with Couplings*, J. R. Stat. Soc., B: Stat. Methodol., 82 (2020), pp. 543–600.
- [20] R. R. LAM, O. ZAHM, Y. M. MARZOUK, AND K. E. WILLCOX, *Multifidelity dimension reduction via active subspaces*, SIAM Journal on Scientific Computing, 42 (2020), pp. A929–A956.
- [21] M. B. LYKKEGAARD, T. J. DODWELL, C. FOX, G. MINGAS, AND R. SCHEICHL, *Multilevel Delayed Acceptance MCMC*, SIAM/ASA J. Uncertainty Quantification, 11 (2023), pp. 1–30.
- [22] J. P. MADRIGAL CIANCI, *Hierarchical Markov chain Monte Carlo methods for Bayesian inverse problems*, PhD thesis, EPFL, Lausanne, 2022.
- [23] J. P. MADRIGAL-CIANCI, F. NOBILE, AND R. TEMPONE, *Analysis of a Class of Multilevel Markov Chain Monte Carlo Algorithms Based on Independent Metropolis–Hastings*, SIAM/ASA J. Uncertainty Quantification, 11 (2023), pp. 91–138.
- [24] B. L. NELSON, *Control variate remedies*, Operations Research, 38 (1990), pp. 974–992.
- [25] F. NOBILE AND F. TESEL, *A multi level monte carlo method with control variate for elliptic pdes with log-normal coefficients*, Stochastic Partial Differential Equations: Analysis and Computations, 3 (2015), pp. 398–444.
- [26] J. O’LEARY AND G. WANG, *Metropolis–Hastings transition kernel couplings*, ANN I H POINCARÉ PR., 60 (2024), pp. 1101 – 1124.
- [27] M. D. PARNO AND Y. M. MARZOUK, *Transport map accelerated markov chain monte carlo*, SIAM/ASA J. Uncertainty Quantification, 6 (2018), pp. 645–682.
- [28] B. PEHERSTORFER AND Y. MARZOUK, *A transport-based multifidelity preconditioner for markov chain monte carlo*, Adv Comput Math, 45 (2019), pp. 2321–2348.
- [29] B. PEHERSTORFER, K. WILLCOX, AND M. GUNZBURGER, *Survey of Multifidelity Methods in Uncertainty Propagation, Inference, and Optimization*, SIAM Rev., 60 (2018), pp. 550–591.
- [30] T. PHAM AND A. A. GORODETSKY, *Ensemble approximate control variate estimators: Applications to multifidelity importance sampling*, SIAM/ASA Journal on Uncertainty Quantification, 10 (2022), pp. 1250–1292.
- [31] R. L. PINTO AND R. M. NEAL, *Improving markov chain monte carlo estimators by coupling to an approximating chain*, tech. report, Technical Report, 2001.
- [32] C. P. ROBERT AND G. CASELLA, *Monte Carlo Statistical Methods*, Springer Texts in Statistics, Springer New York, 2004.
- [33] J. S. ROSENTHAL ET AL., *Optimal proposal distributions and adaptive mcmc*, Handbook of Markov Chain Monte Carlo, 4 (2011).
- [34] H. THORISSON, *Coupling*, Springer New York, New York, NY, 1998, pp. 319–339.
- [35] C. VILLANI ET AL., *Optimal transport: old and new*, vol. 338, Springer, 2009.